

# Third-order nonlinearity of Er<sup>3+</sup>-doped lead phosphate glass

C.C. Santos · I. Guedes · J.P. Siqueira · L. Misoguti ·  
S.C. Zilio · L.A. Boatner

Received: 28 September 2009 / Revised version: 19 January 2010 / Published online: 2 March 2010  
© Springer-Verlag 2010

**Abstract** The third-order optical susceptibility and dispersion of the linear refractive index of Er<sup>3+</sup>-doped lead phosphate glass were measured in the wavelength range between 400 and 1940 nm by using the spectrally resolved femtosecond Maker fringes technique. The nonlinear refractive index obtained from the third-order susceptibility was found to be five times higher than that of silica, indicating that Er<sup>3+</sup>-doped lead phosphate glass is a potential candidate to be used as the base component for the fabrication of photonic devices. For comparison purposes, the Z-scan technique was also employed to obtain the values of the nonlinear refractive index of Er<sup>3+</sup>-doped lead phosphate glass at several wavelengths, and the values obtained using the two techniques agree to within 15%.

## 1 Introduction

Trivalent rare-earth ions can be readily incorporated into a wide range of glass types and compositions to produce

active-optical devices such as solid-state lasers and optical fibers, and the ease with which large optical components can be fabricated from these materials has previously led to numerous studies of the optical properties of rare-earth-doped glasses. In addition to knowing the optical absorption and emission spectra, knowledge of both the linear ( $n_0$ ) and nonlinear ( $n_2$ ) refractive indices is required for the development of optical devices. Specifically, the linear refractive index profile is required to fabricate lenses, planar waveguides, and optical fibers. Additionally, the ability to focus the energy of high-power lasers is limited by self-focusing and beam breakup effects that arise from the intensity-dependent (nonlinear) refractive index changes in optical materials through which a laser beam propagates. The suitability of a laser host material to produce ultra-short pulses generated by the Kerr-lens mode-locking technique [1] is also related to the value of its nonlinear refractive index—i.e., a high value of  $n_2$  corresponds to a more efficient Kerr-lens mode-locking process.

Er<sup>3+</sup>-doped glasses emit infrared fluorescence near 1530 nm through the transition  $^4I_{13/2} \rightarrow ^4I_{15/2}$  that has been extensively investigated for applications in fiber optic communications. Also, green (550 nm) and red (620 nm) up-conversion luminescence can result from the  $^4S_{3/2} \rightarrow ^4I_{15/2}$  and  $^4F_{9/2} \rightarrow ^4I_{15/2}$  transitions, respectively, and there is currently an increasing level of interest in visible optical devices that can be applied in color displays, sensors, optical data storage, bar-code reading, laser printing, and biomedical instrumentation [2–4].

When compared to other oxide glasses (e.g., silicates and borates), phosphate glasses are able to accommodate higher concentrations of rare-earth ions and still remain amorphous. Usually, Er<sup>3+</sup>-doped fiber amplifiers utilize approximately 20 m of silica fiber doped with a few hundred ppm-weight Er<sup>3+</sup> ions [5]. For integrated devices the fiber active

C.C. Santos · I. Guedes (✉)  
Departamento de Física, Universidade Federal do Ceará,  
Campus do PICI, Caixa Postal 6030, 60455-760, Fortaleza, CE,  
Brazil  
e-mail: [guedes@fisica.ufc.br](mailto:guedes@fisica.ufc.br)  
Fax: +55-85-33669450

J.P. Siqueira · L. Misoguti · S.C. Zilio  
Instituto de Física de São Carlos, Universidade de São Paulo,  
13560-970 São Carlos, SP, Brazil

L.A. Boatner  
Center for Radiation Detection Materials and Systems, Materials  
Science and Technology Division, Oak Ridge National  
Laboratory, Oak Ridge, TN 37831-6056, USA

length should be reduced to a few centimeters. This could be attained by increasing the  $\text{Er}^{3+}$  doping concentration. However, a larger  $\text{Er}^{3+}$  concentration in silica glass results in concentration quenching caused by ion clusters [6]. Phosphate glasses, however, can incorporate more than a 2 wt% of  $\text{Er}^{3+}$  doping concentration without such quenching, and the addition of ions such as Sc or rare-earth ions also increases the chemical durability of lead phosphate glasses [7–10]. Additionally, the incorporation of lead atoms in a phosphate glass matrix can be used to increase both the  $n_0$  and  $n_2$  refractive indices, and high values of  $n_0$  and  $n_2$  are needed for the manufacture of holey fibers [11, 12].

In this work we report the experimental determination of  $n_0$  and  $n_2$  for an  $\text{Er}^{3+}$ -doped lead phosphate glass. The spectrally resolved femtosecond Maker fringes technique was also used to determine both the magnitude of the cubic nonlinearity,  $\chi^{(3)}$ , which is related to  $n_2$ , and the dispersion of  $n_0$  (400–1940 nm). For comparison purposes, we have also used the sensitive Z-scan technique to determine  $n_2$  at several wavelengths.

## 2 Experimental

The Er-doped lead phosphate (EDLP) glass was prepared from charges consisting of lead hydrogen phosphate,  $\text{PbHPO}_4$ , to which an appropriate amount of  $\text{ErCl}_3$  was added. The lead hydrogen phosphate was initially prepared by chemically precipitating  $\text{PbHPO}_4$  from a lead nitrate solution by adding phosphoric acid. Upon heating, the  $\text{PbHPO}_4$  decomposes to form lead pyrophosphate,  $\text{Pb}_2\text{P}_2\text{O}_7$ , which then combines with the erbium dopant. The glass was prepared by melting the starting composition in a platinum crucible and then pouring the melt at 950°C into a heated (430°C) graphite mold. The glass was subsequently annealed in air at 430°C for 24 hours and then cut with a diamond saw and optically polished. The final sample thickness was 1.1 mm. The starting composition of the sample consisted of 30 g of  $\text{PbHPO}_4$  plus 0.6 g of  $\text{ErCl}_3$ , resulting in an  $\text{Er}^{3+}$  concentration of about  $2.5 \times 10^{19}$  ions/cm<sup>3</sup>, as confirmed by quantitative chemical analysis performed at the Galbraith Laboratories, Inc. (Lab. ID H-0666-70). The total halogen retained as Cl in the glass was less than 210 ppm. The glass density, determined by the Archimedes method, was found to be 5.1 g/cm<sup>3</sup>. The glass characteristics are summarized in Table 1.

The linear absorption spectra in the wavelength range from 350 to 1700 nm were measured with a commercial double-beam spectrophotometer. The light source for the nonlinear experiments (spectrally resolved Maker fringes and Z-scan) was an optical parametric amplifier pumped with Ti:sapphire amplified laser. Light pulses (10 nm bandwidth) of  $\approx 120$  fs duration at a 1 kHz repetition rate were utilized.

**Table 1** Characteristics and designation of the  $\text{Er}^{3+}$ -doped lead phosphate glass (EDLP). wt% is the nominal doping concentration, the density ( $\rho$ ) was determined by the Archimedes method,  $N_{\text{Er}}$  is the calculated concentration, and  $l$  is the sample thickness

Designation	$\text{ErCl}_3$ (wt%)	$\rho$ (g/cm <sup>3</sup> )	$N_{\text{Er}}$ ( $\times 10^{20}$ ions/cm <sup>3</sup> )	$l$ (mm)
EDLP	2	5.0955	0.25	1.11

## 3 Results and discussion

The dependence of the refractive index on the light irradiance is expressed by  $n = n_0 + n_2 I$ , where  $I$  is the beam irradiance in units of W/m<sup>2</sup>,  $n_0$  is the linear refractive index of the material, and the coefficient of proportionality  $n_2$  is the nonlinear refractive index, which is known to be proportional to  $\chi^{(3)}$ , as discussed later.

For ion-doped systems the pumping of the upper laser level also contributes to the nonlinearity of the refractive index through heat generation and the difference between the excited- and ground-state polarizabilities. To obtain the cubic nonlinearity arising mainly from electronic effects, it is necessary to excite the sample in the regions of negligible linear absorption [13].

Figure 1 shows the normalized absorption spectrum obtained for EDLP glass. The sharp bands are assigned to the 4f–4f transitions of the  $\text{Er}^{3+}$  ions, from the ground state  $^4\text{I}_{15/2}$  to the excited states:  $^4\text{I}_{13/2}$  (1540 nm),  $^4\text{I}_{11/2}$  (977 nm),  $^4\text{I}_{9/2}$  (796 nm),  $^4\text{F}_{9/2}$  (655 nm),  $^4\text{S}_{3/2}$  and  $^4\text{H}_{11/2}$  (547 and 523 nm),  $^4\text{F}_{7/2}$  (490 nm),  $^4\text{F}_{5/2}$  (453 nm),  $^2\text{H}_{9/2}$  (409 nm),  $^2\text{G}_{11/2}$  (379 nm) and  $^2\text{G}_{9/2}$  (367 nm).

Most of the techniques used to measure the linear refractive index are based primarily on optical beam deviation and Snell's law [14], e.g., as manifested in the Abbe and Pulfrich refractometers. Such techniques require precise angle measurements, several monochromatic light sources to characterize the index dispersion, and relatively large size samples. To circumvent this problem, we have used a femtosecond third-harmonic (TH) Maker fringes technique capable of simultaneously providing the magnitude of the cubic nonlinearity,  $|\chi^{(3)}|$ , and the linear refractive index dispersion,  $n_0(\lambda)$ , of optical materials [15]. Briefly, the Maker fringes technique is based on the observation of an oscillatory pattern in the intensity of the TH generated as a function of the incidence angle on the sample. When the TH signal is generated by broadband laser pulses, the fringe pattern cannot be observed due to the dispersion of the sample and the superposition of different patterns produced by wavelengths present within the laser bandwidth. However, this problem can be circumvented by using a spectrometer to de-convolute the TH Maker fringes for different angles of incidence. The oscillatory pattern that is present at each wavelength contains information about the coherence

**Fig. 1** Normalized absorption spectrum of EDLP glass

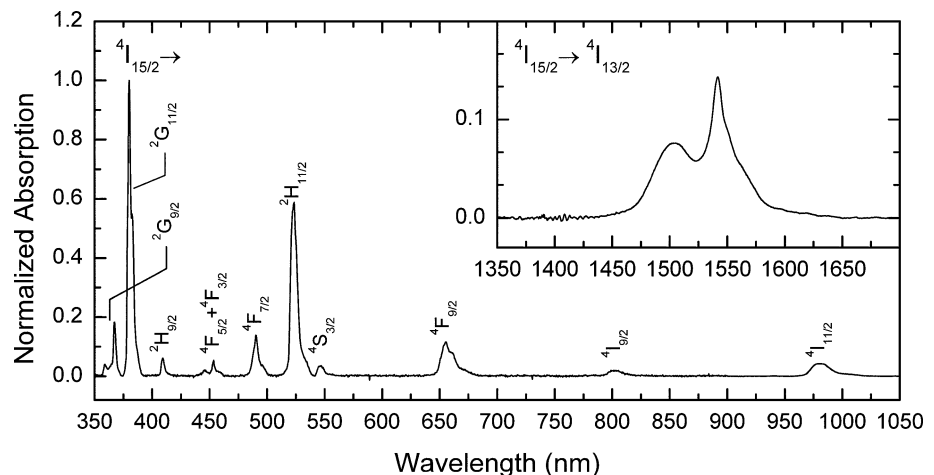
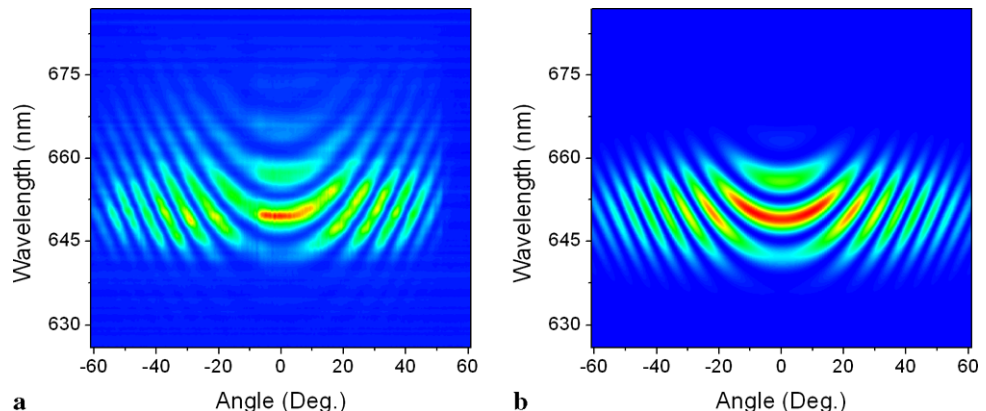


**Fig. 2** Third harmonic Maker fringes for EDLP at 1940 nm.  
**(a)** Experimental and  
**(b)** theoretical patterns



length, which is related to the difference of the refractive index between the fundamental and the TH beams. The curvature of a particular maximum (minimum) of a TH signal band contains information about the refractive index derivative. In other words, the TH Maker fringes process connects the values of the refractive index and its dispersion over two remote wavelength regions.

The procedure used to obtain the dispersion of the refractive index and the Sellmeier coefficients is as follows: (i) First, the TH spectrogram for the EDLP glass is obtained by pumping at 1940 nm, as shown in Fig. 2; and (ii) Second, the TH spectrogram is fit using (1)–(4) of Ref. [15], to obtain the material's refractive index,  $n(\lambda)$ , described by the Sellmeier equation:

$$n^2(\lambda) = 1 + \frac{a\lambda^2}{(\lambda^2 - b)} + \frac{c\lambda^2}{(\lambda^2 - d)} + \frac{e\lambda^2}{(\lambda^2 - f)}. \quad (1)$$

Following the procedure described in Ref. [14], we obtain the following coefficients of the Sellmeier equation:  $a = 1.479$ ,  $b = 0.0192 \mu\text{m}^2$ ,  $c = 0.385$ ,  $d = 0.012 \mu\text{m}^2$ ,  $e = 0.924$  and  $f = 107.14 \mu\text{m}^2$ . Several pump wavelengths at 1570, 1700, 1800 and 1870 nm were used to obtain a more accurate value of the Sellmeier coefficients.

An optical glass is usually described by its refractive index at the helium  $d$  line (587.6 nm),  $n_d$ , and the Abbe number,  $v_d$ , which characterizes the dispersion. The Abbe number is given by  $v_d = (n_d - 1)/(n_F - n_C)$ , where  $n_F$  and  $n_C$  are respectively the refractive indices for reference lines of hydrogen:  $F$  (486.1 nm) and  $C$  (656.3 nm). Using (1) and the values determined for the Sellmeier coefficients we find  $n_d = 1.721$ ,  $n_F = 1.736$ ,  $n_C = 1.715$ , and  $v_d = 34$ .

The nonlinear refractive index can be roughly estimated from the values of  $n_d$  and  $v_d$  by using the following expression [16]:

$$n_2[\text{m}^2/\text{W}] = 2.85 \times 10^{-18} \times \frac{(n_d - 1)(n_d^2 + 2)^2}{n_d v_d \sqrt{1.517 + (n_d^2 + 2)(n_d + 1)v_d/6n_d}} \quad (2)$$

which yields a value of  $n_2 = 1.27 \times 10^{-19} \text{ m}^2/\text{W}$  for the EDLP glass. This value reflects the fact that a high  $n_2$  is expected for glasses with a high  $n_0$  ( $\sim n_d$ ) and a low Abbe number. From the Abbe diagram ( $n_d \times v_d$ ) we observe that the following relation frequently holds:  $n_2$  (fluorides)  $< n_2$  (oxides).

(oxides) <  $n_2$  (silicates) <  $n_2$  (phosphates) <  $n_2$  (chalco-genides) [17].

The Maker fringes technique measures the fast, electronic part of the cubic susceptibility,  $\chi^{(3)}(3\omega; \omega, \omega, \omega)$ , while the Z-scan technique measures the nonlinear refractive index, which is related to the global Kerr susceptibility,  $\chi^{(3)}(\omega; \omega, -\omega, \omega)$ . As recently shown by Rau et al. for silica ( $\text{SiO}_2$ ), the relation  $\chi^{(3)}(3\omega; \omega, \omega, \omega) \sim \chi^{(3)}(\omega; \omega, -\omega, \omega)$  holds [18]. Therefore, an estimate of the  $n_2$  value can be obtained from the TH measurements through the following equation [19]:

$$n_2[\text{m}^2/\text{W}] = \frac{120\pi^2}{n_0^2 c} \chi^{(3)}[\text{esu}], \quad (3)$$

where  $c$  is the speed of light in units of m/s, and it can then be compared to the value obtained with Z-scan measurements.  $\chi^{(3)}(3\omega; \omega, \omega, \omega)$  is determined by comparing the TH intensity with that of a reference sample that, in this case, is a 600  $\mu\text{m}$ -thick  $\text{SiO}_2$  slab ( $\chi_{\text{SiO}_2}^{(3)} = 2.0 \times 10^{-14}$  esu [20]). This is accomplished by measuring the integrated spectral intensity using a large-area broadband detector and a lock-in amplifier. Following the procedure described in Ref. [15], we obtain for the EDLP glass at a wavelength of 1700 nm,  $\chi^{(3)} = 1.3 \times 10^{-13}$  esu, and from (3), we obtain:  $n_2 = 1.8 \times 10^{-19} \text{ m}^2/\text{W}$ . This value is about 40% higher than that predicted by (2) which uses the linear parameters  $n_d$  and  $v_d$ . The EDLP glass exhibits a TH generation efficiency 6.5 times higher than that of  $\text{SiO}_2$ .

The value of  $n_2$  achieved by using the TH Maker fringes technique can be compared with that obtained through the use of the sensitive transmission Z-scan technique [21] that is based on the transmittance measurement through a finite aperture placed at the far field as a function of the nonlinear sample position,  $z$ , with respect to the focal plane. A quantity  $\Delta T_{p-v}$ , defined as the difference between the normalized peak (maximum) and valley (minimum) transmittances is easily measurable and is given as a function of the average phase distortion  $\Delta\Phi_0$  as:

$$\Delta T_{p-v} \approx p |\Delta\Phi_0| \quad (4)$$

for  $|\Delta\Phi_0| \leq \pi$ , where  $p = 0.406(1 - S)^{0.25}$ ,  $S$  is the aperture transmittance, and  $\Delta\Phi_0$  is defined as:

$$\Delta\Phi_0 = (2\pi/\lambda)n_2 I_0 L_{\text{eff}}, \quad (5)$$

where  $\lambda$  is the laser wavelength,  $I_0$  is the on-axis irradiance at the focus ( $z = 0$ ),  $L_{\text{eff}} = (1 - e^{-\alpha L})/\alpha$  is the effective length—with  $L$  being the sample length and  $\alpha$  the linear absorption coefficient.

It is well known that the main source of uncertainty in the value of  $n_2$  is the absolute measurement of the irradiance. With ultra-short pulses, it is also important to account for

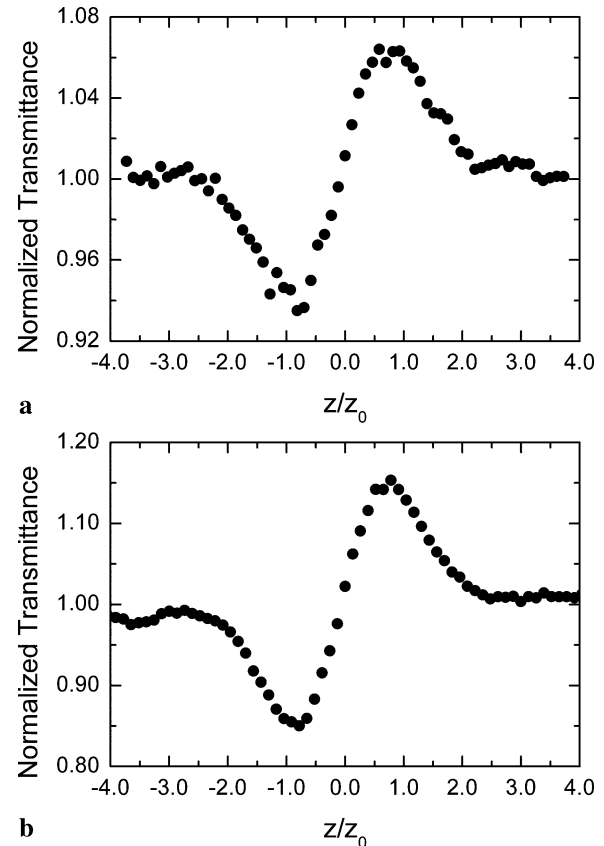


**Fig. 3** Results of Z-scan measurements at 1700 nm for (a)  $\text{SiO}_2$  and (b) EDLP

a possible increase of the pulse duration due to the group velocity dispersion (GVD) in the sample, which alters the peak irradiance and, hence, the magnitude of the nonlinear phase shift. Using a reference sample ( $\text{SiO}_2$ ) with a well-known  $n_2$  value ( $0.37 \times 10^{-19} \text{ m}^2/\text{W}$  [18]) reduces such uncertainty and gives us the value of the irradiance to be used in (5).

The Z-scan trace for  $\text{SiO}_2$  and EDLP at 1700 nm is shown in Fig. 3(a) and (b), respectively. Neither a linear nor two-photon absorption was observed, indicating that the nonlinear refraction arises mainly from the electronic Kerr effect. The valley-peak profile of the Z-scan signals indicates a positive sign of  $n_2$ . From (4) and (5) with  $\alpha = 10 \text{ m}^{-1}$  (the lowest value detectable) and  $S \sim 0$ , we obtain  $n_2 = 1.6 \times 10^{-19} \text{ m}^2/\text{W}$ . The ratio  $n_2(\text{Z-scan})/n_2(\text{THG}) \sim 0.89$  is of the same order as that found in Ref. [18] for  $\text{SiO}_2$ , indicating that for glasses, the relation  $\chi^{(3)}(3\omega; \omega, \omega, \omega) \sim \chi^{(3)}(\omega; \omega, -\omega, \omega)$  holds. The value of  $n_2$  can also be used to calculate the figure of merit  $W = (n_2 I / \lambda \alpha)$  [22], which for all-optical switching is required to be  $W \gg 1$ . For the EDLP glass, we find (with  $I = 1.11 \times 10^{15} \text{ W/m}^2$ )  $W = 10.45$  at 1700 nm.

We have also used the Z-scan technique to measure  $n_2$  at several wavelengths in the visible region. The values found

are:  $1.70 \times 10^{-19} \text{ m}^2/\text{W}$  at 600 nm,  $2.00 \times 10^{-19} \text{ m}^2/\text{W}$  at 640 nm,  $1.85 \times 10^{-19} \text{ m}^2/\text{W}$  at 680 nm, and  $2.00 \times 10^{-19} \text{ m}^2/\text{W}$  at 720 nm. The nonmonotonic behavior of  $n_2$  is mainly due to the laser intensity fluctuation ( $\sim 20\%$ ) in this wavelength region. However, as shown in Ref. [23] the dispersion of  $n_2$  resembles that of the linear refractive index, i.e.,  $n_2$  decreases as  $\lambda$  increases.

In spite of the low values of  $n_0$  ( $\sim 1.44$ ) and  $n_2$  ( $0.2-0.4 \times 10^{-19} \text{ m}^2/\text{W}$ ), SiO<sub>2</sub>-based glasses are still largely used in the fabrication of photonic materials and as photonic crystal fibers (PCFs). Despite their availability and good optical performance in the visible/near-infrared, silica glasses have high melting points ( $\sim 1600^\circ\text{C}$ ). Accordingly, the search for materials with lower melting points and higher  $n_0$  and  $n_2$  values can make the tailoring of new complex air-glass structures possible. Recently, two papers have reported on the potential use of non-silica glasses with lower melting points in the fabrication of PCFs [24, 25]. In Ref. [24], Lorenc et al. used the Z-scan technique to obtain the  $n_2$  values of various multi-component glasses. The values of the linear and nonlinear refractive index span the range 1.5 up to 2.4 and 0.11 up to  $4.3 \times 10^{-19} \text{ m}^2/\text{W}$ , respectively. In Ref. [25], Feng et al. used (2) to determine  $n_2$  for high-lead silicate glasses (commercial Schott SF57 and SF59), tellurite and gallium lanthanum chalcosulfide glasses.

For the EDLP, glass the melting point is around  $950^\circ\text{C}$  and,  $n_2 \sim 1.6-2.0 \times 10^{-19} \text{ m}^2/\text{W}$ , on average. We observed that the  $n_2$  value for EDLP is similar to that of F7 and SF6 glasses [25] for which holey fiber production has been demonstrated. This indicates that EDLP glasses may be used as the base material in the fabrication of PCFs.

#### 4 Conclusion

We have used the spectrally resolved femtosecond Maker fringes technique to obtain the absolute value of  $\chi^{(3)}$  and the dispersion of  $n_0$  for EDLP glass in the 300 to 1940 nm range. From the Sellmeier equation, we obtained the values of  $n_d$ ,  $n_F$ ,  $n_C$  and the  $v_d$ . The low value of  $v_d = 34$  indicates that the EDLP glass is a dispersive glass as evidenced by the observation of narrow fringes as shown in Fig. 2. Also, we have used the sensitive transmission Z-scan technique to determine the value of  $n_2$  for the EDLP glass at different wavelengths. No nonlinear absorption was observed. The values found for  $n_2$  at 1700 nm using both the Z-scan and THG methods were  $1.6 \times 10^{-19} \text{ m}^2/\text{W}$  and  $1.8 \times 10^{-19} \text{ m}^2/\text{W}$ , respectively. As compared to silica glass, the EDLP glass exhibits larger values of  $n_0$  ( $> 25\%$ ) and  $n_2$  ( $\sim 500\%$ ), and therefore, it is a candidate for use as a base material for tailoring optical devices.

**Acknowledgements** The financial support for this research by the FUNCAP, CAPES, PRONEX, FAPESP, CNPq and FINEP Brazilian agencies is gratefully acknowledged. The research was sponsored in part by the Division of Materials Sciences and Engineering, Office of Basic Energy Sciences, U.S. Department of Energy, under Contract No. DE-AC05-00OR2725 with Oak Ridge National Laboratory managed and operated by UT-Battelle, LLC.

#### References

1. D.E. Spence, P.N. Kean, W. Sibbett, Opt. Lett. **16**, 42 (1991)
2. W.P. Risk, T.R. Gosnell, A.V. Nurmikko, *Compact Blue-Green Lasers* (Cambridge University Press, Cambridge, 2003)
3. G. Blasse, B.C. Grabmaier, *Luminescent Materials* (Springer, Berlin, 1994)
4. B. Karmakar, R.N. Dwivedi, J. Non-Cryst. Solids **342**, 132 (2004)
5. M. Shimizu, M. Yamada, M. Horiguchi, E. Sugita, IEEE Photonics Technol. Lett. **2**, 43 (1990)
6. R.S. Quimby, W.J. Miniscalco, B. Thompson, J. Appl. Phys. **76**, 4472 (1994)
7. Y.C. Yan, A.J. Faber, H. de Waal, P.G. Kik, A. Polman, Appl. Phys. Lett. **71**, 2922 (1997)
8. J. Schmulovich, in *Rare-Earth-Doped Devices* (SPIE, San Jose, 1997), p. 143
9. K.A. Winick, in *Rare-Earth-Doped Devices II* (SPIE, San Jose, 1998), p. 88
10. B.C. Sales, L.A. Boatner, J. Am. Ceram. Soc. **70**, 615 (1987)
11. P. Petropoulos, T.M. Monro, H. Ebendorff-Heidepriem, K. Frampton, R.C. Moore, H.N. Rutt, D.J. Richardson, in *Optical Fiber Communications Conference, 2003. OFC 2003*, p. PD3
12. T.M. Monro, K.M. Kiang, J.H. Lee, K. Frampton, Z. Yusoff, R. Moore, J. Tucknott, D.W. Hewak, H.N. Rutt, D.J. Richardson, in *Optical Fiber Communication Conference and Exhibit, 2002. OFC 2002*, p. FA1
13. A.A. Andrade, T. Catunda, R. Lebrellenger, A.C. Hernandes, M.L. Baesso, J. Non-Cryst. Solids **273**, 257 (2000)
14. M. Born, E. Wolf, *Principles of Optics: Electromagnetic Theory of Propagation, Interference and Diffraction of Light* (Cambridge University Press, Cambridge, 1999)
15. I.A. Heisler, L. Misoguti, S.C. Zilio, E.V. Rodriguez, C.B. de Araujo, Appl. Phys. Lett. **92**, 091109 (2008)
16. S. Hazarika, S. Rai, Opt. Mater. **30**, 462 (2007)
17. H. Bach, N. Neuroth, *The Properties of Optical Glass* (Springer, New York, 1998)
18. I. Rau, F. Kajzar, J. Luc, B. Sahraoui, G. Boudebs, J. Opt. Soc. Am. B **25**, 1738 (2008)
19. R.W. Boyd, *Nonlinear Optics* (Academic Press, San Diego, 2003)
20. G.R. Meredith, B. Buchalter, C. Hanzlik, J. Chem. Phys. **78**, 1533 (1983)
21. M. Sheik-Bahae, A.A. Said, T.H. Wei, D.J. Hagan, E.W. Vanstryland, IEEE J. Quantum Electron. **26**, 760 (1990)
22. G.I. Stegeman, in *Nonlinear Optics of Organic Molecules and Polymers*, ed. by H.S. Nalwa, S. Miyata (CRC Press, Boca Raton, 1997), p. 799
23. A. Major, I. Nikolakakos, J.S. Aitchison, A.I. Ferguson, N. Langford, P.W.E. Smith, Appl. Phys. B, Lasers Opt. **77**, 433 (2003)
24. D. Lorenc, M. Aranyosiova, R. Buczynski, R. Stepien, I. Bugar, A. Vincze, D. Velic, Appl. Phys. B, Lasers Opt. **93**, 531 (2008)
25. M. Feng, A.K. Mairaj, D.W. Hewak, T.M. Monro, J. Lightwave Technol. **23**, 2046 (2005)